# Efficient Growth of Vertically-Aligned Single-Walled Carbon Nanotubes with Combining Two Unfavorable Synthesis Conditions

Ming Liu[1], Hua An[1], Akihito Kumamoto[2], Taiki Inoue[1], Shohei Chiashi[1], Rong Xiang[1] *, Shigeo Maruyama[1,3] *

[1] *Department of Mechanical Engineering, The University of Tokyo, Tokyo 113-8656, Japan*

[2] *Institute of Engineering Innovation, The University of Tokyo, Tokyo 113-8656, Japan*

[3] *Energy Nano Engineering Lab., National Institute of Advanced Industrial Science and Technology (AIST), Tsukuba 305-8564, Japan*

Correspondence may be addressed:

xiangrong@photon.t.u-tokyo.ac.jp (R. X.); maruyama@photon.t.u-tokyo.ac.jp (S. M.)

**Abstract**

We demonstrate an unexpected recipe for the efficient synthesis of vertically-aligned single-walled carbon nanotubes (SWCNTs). The growth of high density arrays is achieved by combining two unfavorable conditions: low temperature and mono-metallic Co catalyst, neither of which was previously found to be effective for the synthesis of SWCNT forest. As the result of this new recipe, the as-synthesized SWCNTs have a narrower diameter distribution than those obtained in previous studies, with 85% of the SWCNTs between 1.6 and 2.4 nm. Meanwhile, we utilize our recently established transmission electron microscopy (TEM) technique to characterize this monometallic Co catalyst directly on $SiO_2$. Nanoparticles in a 600°C reaction are confirmed to be smaller, denser and more uniform than those formed at high temperatures. Our technique further allows to image catalyst at high temperatures, by which Ostwald ripening is visualized at a single particle level. In addition, *in situ* electron diffraction and imaging confirm that monometallic Co catalyst remains as solid phase even at 800°C. The discovery of new growth recipe increases the compatibility of synthesizing SWCNT onto other substrates. The new TEM technique provides experimental evidence for some long-standing hypotheses of catalytic particles and is capable of guiding the design of new catalyst.

## 1. Introduction

Single-walled carbon nanotubes (SWCNTs) have received much attention over the past few decades due to their unique chiral structures and interesting electronic, thermal, and mechanical properties [1-3]. One interesting macroscopic geometry of SWCNTs is the forest-like vertically-aligned array, which was first synthesized in early 2004 [4] using alcohol catalytic chemical vapor deposition (ACCVD) [5]. The production of vertically aligned SWCNT (VA-SWCNT) arrays was an important breakthrough in the synthesis of SWCNT assemblies as it offered a way to yield high-density SWCNTs with an identical orientation. Immediately after this, a scaled up production technique was developed [6].

Though vertically aligned SWCNT array possesses many interesting properties, synthesizing such a structure usually requires severe reaction conditions. The first is the unique design of catalyst. Among the many types of catalyst that had been explored in the past decades, only two options, Co-Mo and Fe-Al, are found to be capable of reproducibly synthesizing VA-SWCNT arrays [4, 6]. In these two bimetallic combinations, the empirical understanding is that Co (or Fe) serves as the active site, while Mo (or Al) is a stabilizer which keeps active sites stable and uniformly dispersed [7]. Monometallic catalyst, e.g. pure Co (or Fe), is seldom found to be effective to yield VA-SWCNT arrays. In most of the cases, only multi-walled carbon nanotubes (MWNTs) or very sparse SWCNTs are obtained [8, 9].

Another severe condition for VA-SWCNT production is the requirement of high reaction temperature. The synthesis of millimeter-tall VA-SWCNTs from Co and $Al_2O_x$ binary catalyst was performed at temperature higher than 850°C [10]. The water-assisted CVD process of producing VA-SWCNTs arrays from Fe and $Al_2O_3$ catalysts is conducted at 750°C[11, 12]. The synthesis of VA-SWCNT forest in our previous work is usually performed at 800°C [13]. A slight decrease of operation temperature for bimetallic Co and Cu catalysts could cause a significant drop of SWCNT yield [14]. Reducing the reaction temperature while keeping the forest geometry has been a great challenge.

Due to the requirement of high reaction temperature, the necessity of using a bimetallic combination is usually attributed to the difficulty of controlling the size of monometallic catalyst at high temperatures. For the growth of MWNTs, the size of catalyst particles usually above 10 nm [15-17], whereas SWCNT growth requires the catalyst to be only 1-

3 nm [18-20]. At this scale, thermal sintering at elevated temperatures becomes crucial, which can lead to the increase of average particle size and the broadening of size distribution [21]. Previous studies on particle sintering suggested temperature is one of key factors here. Ruckenstein and Pulvermacher revealed that the decay of an exposed metal surface area during heat treatment relates to the mobility of the crystallites on the support and the merging rate of two colliding particles into a single particle [22]. Baker suggested that the onset of mobility occurred at the Tammann temperature ($0.5\,T_{\mathrm{melting}}^{\mathrm{bulk}}$[K]), where surface atoms become mobile and constitutes the mechanism for particle mobility [23]. In this theory, a reduction of the CVD temperature, i.e., reducing catalyst mobility, may be a promising approach to control the diameters of catalyst nanoparticles and narrow the distribution of the diameters of as-synthesized SWCNT. However, as previously noted, the reduction of growth temperature usually results in a significant sacrifice of catalytic efficiency in case of bimetallic catalyst.

While recognizing neither "low temperature" nor "monometallic catalyst" as an efficient strategy for SWCNT production, the community had paid little attention to the behavior of monometallic catalyst under low reaction temperatures. Recently, we revisited many monometallic catalysts and re-investigated their size, crystallization, chemical states and others using newly developed transmission electron microscopy (TEM) technique [24]. In that work, a regularly high temperature (800ºC) was used and yield of SWCNTs was low. Here, when reducing the reaction temperature, we present a possibility of synthesizing VA-SWCNT arrays with a narrow diameter distribution using a new recipe. This recipe combines the monometallic Co catalyst with a low CVD temperature, 600ºC. Furthermore, we employ our recently established in-plane TEM technique [24] to characterize this low temperature formed monometallic Co catalyst nanoparticles. Ostwald ripening in the monometallic Co nanoparticles is directly observed at single particle level. VA-SWCNT arrays with narrow diameter distributions are expected to improve the performance of SWCNTs particularly for applications in photoelectric devices and filtration.

## 2. Experimental methods

The Co catalyst (nominal thickness 0.3 nm) was deposited on a 500 μm thick Si substrate with a 100 nm thick thermally grown $SiO_2$ layer (SUMCO) by magnetron

sputtering (Ulvac-Riko), followed by annealing at 400°C in air for 5 min to break up the catalyst film into particles. VA-SWCNTs were synthesized by ACCVD [4] with a modification to the pre-decomposition of ethanol (left chamber 900°C). Briefly, the substrate supporting the catalyst particles was placed in a quartz tube (2.5 cm diameter) and reduced at a pressure of 40 kPa with the temperature increased from room temperature to 600°C over 15 min and then held at 600°C for another 15 min under an $Ar/H_2$ (3%) atmosphere. After evacuation of the $Ar/H_2$ gas in the tube to a vacuum of 27 Pa, ethanol feedstock (dehydrated, 99.5%, Wako Chemical, Inc.) was introduced at flow rates in the range of 50-450 sccm for a growth period of 5 min.

As-synthesized VA-SWCNTs were characterized using scanning electron microscopy (SEM; Hitachi S-4800) at an accelerating voltage of 1 kV. Raman spectra were measured using a Renishaw inVia Raman system with excitation wavelengths of 488, 532, 633, and 785 nm.

The Co catalyst was directly deposited on a $Si/SiO_2$ TEM grid (20 nm $SiO_2$), which was later transferred into CVD chamber for SWCNT synthesis. After the CVD process, the grid with catalyst and SWCNTs is used for TEM measurement without any sample pretreatment. This strategy allows us to see the catalyst and is able to characterize the SWCNTs in the original morphology. TEM images were obtained with a JEM-2000EX-II microscope and atomic resolution images were obtained with a JEM-ARM200F microscope. High-angle annular dark-field scanning TEM (HAADF-STEM) images were obtained by a JEM-ARM200F microscope with a cold field-emission gun using a probe size typically smaller than 0.1 nm. The selected area electron diffraction (SAED) patterns were obtained using the same microscope in a near parallel beam condition. The typical exposure time is around 30 seconds. More details of the direct imaging on a $Si/SiO_2$ TEM grid can be found in our previous report [24]. All the TEMs were operated at an acceleration voltage of 200 kV.

## 3. Results and discussion

### 3.1 Characterizations of the narrow-diameter VA-SWCNT forest

Figure 1(a) shows a schematic of a VA-SWCNT array grown on a substrate. The premier of producing such a SWCNT forest is to maintain the nucleation sites in a high

density, therefore SWCNTs can support each other and grow into the same direction. Figure 1(b) is the cross-sectional SEM image of the SWCNT forest obtained from the new recipe. The distinct features here are monometallic Co (other than Co-Mo [13]) is employed as the catalyst and the reaction temperature is reduced from 800 to 600°C. As catalyst is prepared by sputtering, as-synthesized VA-SWCNTs show a highly uniform distribution over the entire substrate (Figure S1a). The height of VA-SWCNTs obtained from Co after 5 min growth is typical around 10 μm, according to high resolution SEM image (Figure 1b). We find the combination of "low temperature + monometallic" is essential for obtaining the SWCNTs forest structure. In control experiments and our previous studies as well, both "low temperature + bimetallic catalyst" and "high temperature + monometallic" are inefficient– only sparse and random SWCNT networks are synthesized on the substrate. Though growing SWCNTs on zeolite supported catalyst in a wide parameter window has been achieved [25], in case of a flat substrate, it is an astonishment that the combination of these two unfavorable conditions results in a decently high yield of VA-SWCNTs.

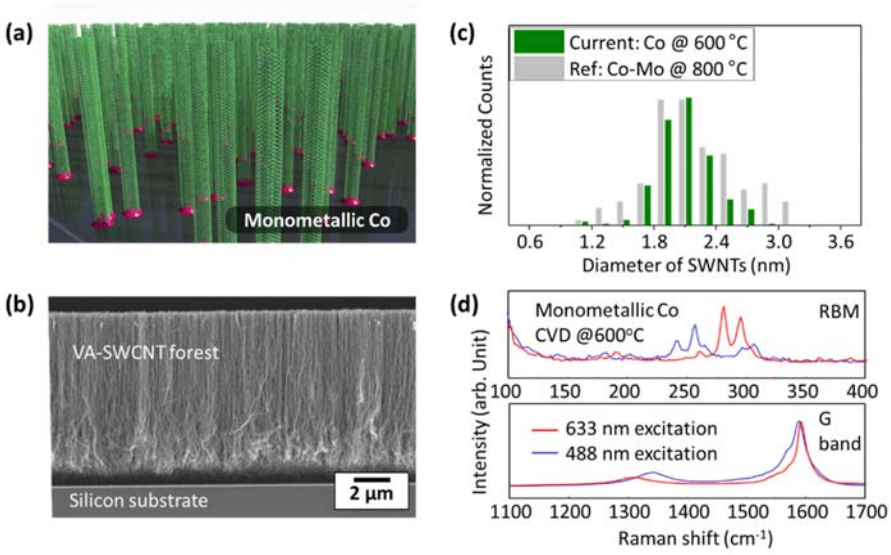


Figure 1. Characterization of as-synthesized VA-SWCNTs. (a) Schematic of a VA-SWCNT forest grown on a substrate; (b) representative cross-sectional SEM image of the VA-SWCNT forest grown from monometallic catalyst at 600°C; (c) diameter distribution of SWCNTs grown from the current new recipe (green) and previous high temperature

process (gray)[26]; (d) Raman spectra measured by laser excitation at 633 nm (red), and 488 nm (blue).

Figure 1c displays the diameter distribution of a typical sample obtained in this study. 85% of the SWCNTs are between 1.6 and 2.4 nm, which is noticeably narrower than our previous sample possessing a similar average diameter [26]. Representative TEM images (Figure S1b) of VA-SWCNT arrays viewed from the top reveals many cross-section of SWCNTs grown perpendicularly to the substrate. The sample contains nearly pure SWCNTs without noticeable amorphous carbon and MWNT impurities. However, high resolution images suggest that there are certain numbers of kinks and buckles.

Raman spectroscopy measurements were performed to confirm the presence of SWCNTs and to characterize the crystallization as well as the diameter of SWCNTs. Fig, 1d shows the resonance Raman spectra for VA-SWCNTs synthesized with the Co catalyst under laser excitation at 488 and 633 nm. The peaks in the radial breathing mode (RBM) region indicate that the current VA-SWCNT sample contains small diameter tubes, in accordance with the RBM ($\omega_{\mathrm{RBM}}$) – SWCNT diameter ($d_t$) relationship: $\omega_{\mathrm{RBM}}$ = 217.8/$d_t$+15.7 [27]. However, this does not reveal the genuine diameter distribution of the sample because of the well-known over-pronunciation of Raman on resonant and small diameter SWCNTs [28] [29]. The average G/D ratio can reach approx. 10, roughly half of the value (20) of our previous samples, as shown in Figure 1d. It is a reasonable quality of SWNTs considering the synthesis temperature is only 600°C.

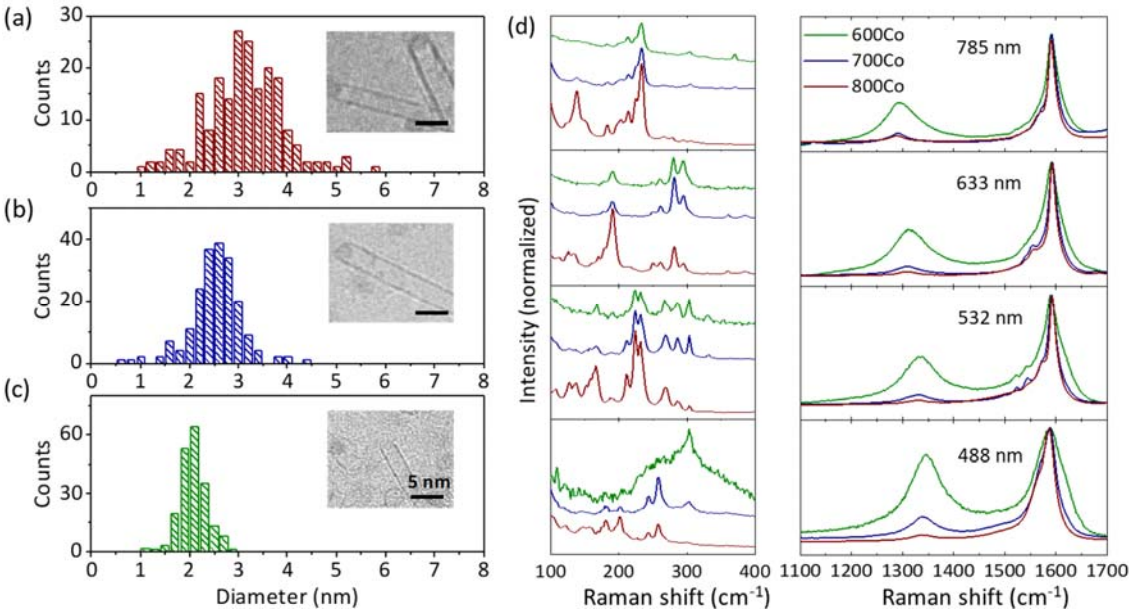


Figure 2. Histograms for the diameters of VA-SWCNTs synthesized at various temperatures; (a) 800°C, (b) 700°C, and (c) 600°C. The insets show representative TEM images of individual SWCNTs. (d) Raman spectra for VA-SWCNTs synthesized at 600°C (600Co), 700°C (700Co), and 800°C (800Co), measured by laser excitations at 488, 532, 633, and 785 nm.

The condition of low reaction temperature contributes to the narrow diameter distribution of the as-produced SWCNTs. A detailed study on the effect of reaction temperature is presented in Figure 2. As clearly seen in Figure 2a-c, the diameter distribution of SWCNTs grown from monometallic Co at different reaction temperatures is distinguishably different. Higher reaction temperature, e.g. 800°C, yields many SWCNTs with diameter larger than 3 nm, while low temperature keeps the diameter small and maintains the diameter within a narrow distribution. Accordingly, the Raman spectra of SWCNTs produced at high temperature also presents much higher RBM peaks within low Raman shift region, which indicates the existence of larger diameter SWCNTs. Meanwhile, the efficiency of this monometallic Co significantly decreases at high temperatures. Only very thin and sparse random SWCNTs are obtained on substrate when the CVD is performed at 800°C, while SWCNTs grow into forests at 600°C, which suggests the catalyst is maintained active at a high density (to estimate later). These observations clearly prove that the combination of

“low temperature” and “monometallic Co” is an unexpected but efficient recipe for the production of VA-SWNTs.

However, one obvious drawback here is that D band peaks of these new SWCNT arrays are relatively higher than the literature works. This relatively higher D band is due to intrinsic defects, e.g. kinks, because we observe no noticeable amorphous carbon in the current sample during our TEM characterizations. We attempt to improve the crystallization of these low temperature synthesized SWCNTs. For our conventional low pressure ACCVD process, the ethanol flow rate used is 450 sccm and the system pressure is 1.3 kPa which are optimized for a reaction temperature of 800°C. However, for this monometallic catalyst low temperature synthesis, crystallization of the VA-SWCNTs is not as good as our conventional samples, according to the D/G ratio shown in Figure 1d. To optimize the growth parameters for this CVD procedure, the ethanol flow rate is therefore decreased from 450 to 250, and 50 sccm. Representative SEM images of the VA-SWCNTs synthesized at different ethanol flow rates are shown in Figure S2, and the corresponding Raman spectra are shown in Figure 3. In the Raman spectra, the RBM regions measured with four different laser excitations showed the diameter distribution was weakly dependent on or independent of the ethanol flow rate, i.e., the diameter and structure of the SWCNTs remained the same as the original sample synthesized at an ethanol flow rate of 450 sccm. However, the D/G ratio of the VA-SWCNTs decreased with the ethanol flow rate; therefore, the crystalline quality of the VA-SWCNTs could be improved without changing the diameter and the geometry of carbon nanotubes. By changing this ethanol flowrate, we could adjust the feeding of carbon source and reduce the growth rate of SWCNTs. A slow growth rate may help to release the strain during growth and reduce the probability of kink formation.

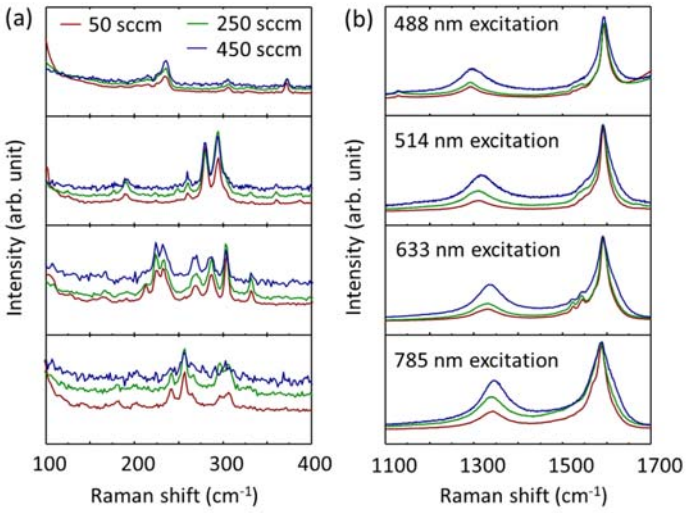


Figure 3. Improving the crystallization of SWCNTs grown at low CVD temperatures. Raman spectra of as-synthesized VA-SWCNTs from ethanol at flow rates of 50, 250, and 450 sccm measured by laser excitation at 488, 532, 633, and 785 nm. (a) RBM and (b) G-band region.

3.2 *Ex situ* and *in situ* TEM characterization of monometallic Co catalyst

Our recent progress allows us to visualize catalyst directly on a thin $SiO_2$ film [14, 24, 30]. Figure 4a-b illustrate the strategy of characterizing the catalyst by using a MEMS fabricated Si/$SiO_2$ TEM grid. In brief, the key of this technique is to employ a $SiO_2$ film that is thin enough to allow electron beam to transmit and also thick enough to support the preparation of catalyst and the growth of SWCNTs. Some more focused discussions can be found in our previous report [24]. Figure 4c presents the SEM image of the original TEM grid used in this experiment. Eight square regions and one rectangle region with 20 nm thickness $SiO_2$ suspended film in the center part serve as the TEM observation windows. Figure 4d and 4e show SEM images of the TEM grid after CVD growth for 8s at 600°C. VA-SWCNTs are uniformly synthesized on the TEM grid including the suspended $SiO_2$ windows. No noticeable differences are found between suspended $SiO_2$ (window) and Si supported $SiO_2$ (substrate) regions. The cross-sectional view of this array in Figure 4e further confirms that the SWCNTs are vertically aligned on the surface of the TEM grid. Figure S3 confirms that the VA-SWCNTs synthesized on a TEM grid are same as the VA-SWNTs produced on a conventional silicon substrate; there is no noticeable difference in

the morphology of arrays and the diameter of VA-SWCNTs according to the representative SEM images and Raman spectra. Figure 4f displays a representative TEM image of the catalyst and SWCNTS obtained directly on $SiO_2$ suspended film. It confirms that monometallic Co forms uniform nanoparticles with a high density, which is essential for the growth of VA-SWCNT arrays. Furthermore, the SAED pattern of the catalyst (Figure 4g) after a 2s CVD also suggests there is no diffraction from the (002) plane of graphite, evidencing the presence of pure SWCNTs. The aberration corrected TEM image in Figure 4h shows that the catalyst particles are mostly single and occasionally twinned crystals. Carbon coating or SWCNT nucleation could be imaged with appropriate focus conditions.

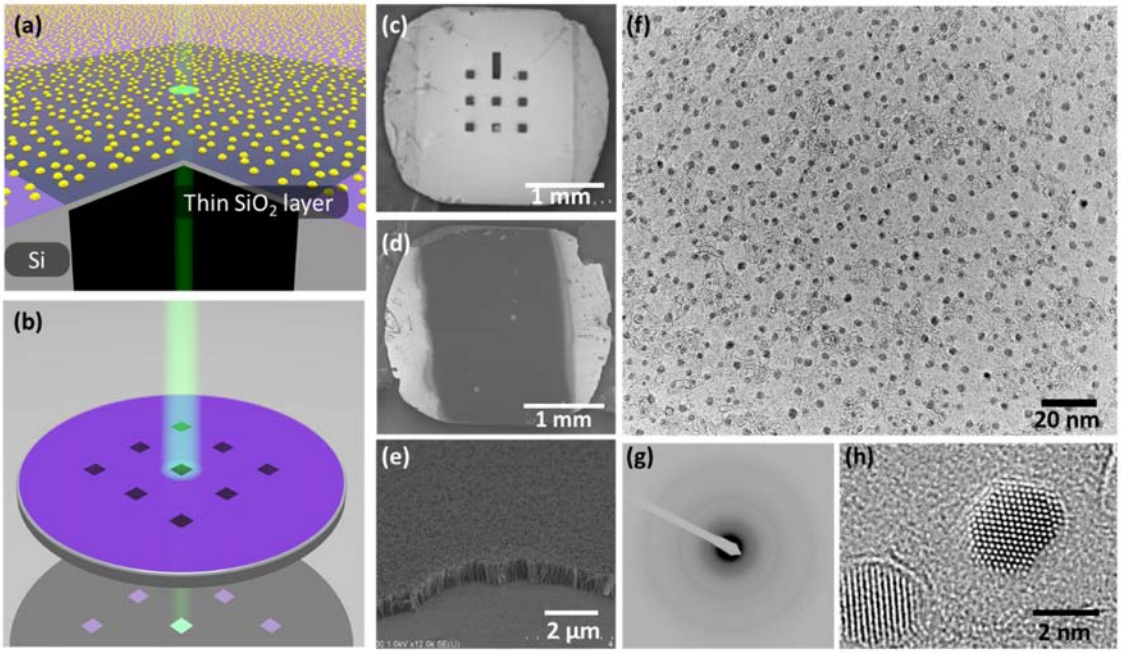


Figure 4. *Ex situ* TEM characterization of the catalytic particles at room temperature. (a)(b) Schematic of the TEM technique used in this study using $Si/SiO_2$ TEM grid; representative SEM image of (c) original $SiO_2/Si$ TEM grid, (d) after growth of VA-SWCNTs on the grid, and (e) cross-sectional view of VA-SWCNTs on the grid. (f) *ex situ* TEM image, (g) SAED pattern, and (h) aberration corrected TEM image of the catalytic Co nanoparticles after CVD for 2 s.

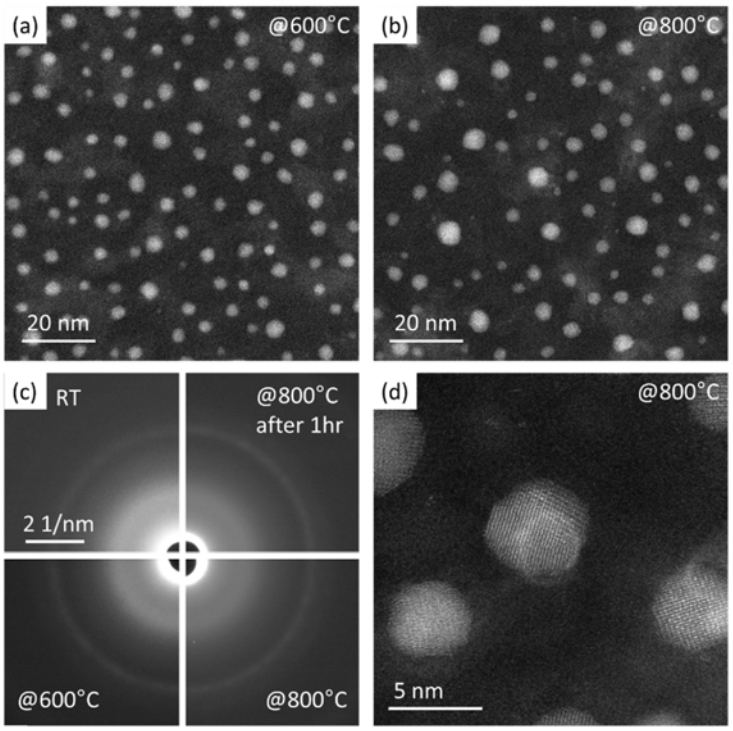


Figure 5 *In situ* STEM characterization of the catalyst at high temperatures. STEM-HAADF image of reduced catalyst at (a) 600°C and (b) 800°C in a heating holder; (c) SAED patterns obtained at different temperatures, revealing no significant change in degree of crystallization; (d) enlarged STEM image of catalytic particles taken at 800°C, evidencing that the particles remain in solid phase.

With this technique, we can directly resolve the differences of catalyst formed at different conditions. Furthermore, *in situ* characterization on the catalyst at high temperatures using, e.g., a heating holder becomes possible by using the $SiO_2$/Si grid. Figure 5 summarizes the information we obtained from *in situ* high temperature characterizations. Figure 5a and 5b display two representative images of the catalyst at 600°C and 800°C obtained by HAADF-STEM, which makes it easier to determine the morphology of metallic Co nanoparticle on the silica thin film due to the *Z*-contrast [14]. In the former case, the particles have relatively uniform size distribution with small diameter and high density. In the latter case, however, some larger diameter particles together with some very small-diameter particles appear, resulting in a broader size distribution. Besides, while counting the number of the particles in a certain area, the

particle density decrease roughly 20-30% in this comparison. Several tens of percentage decrease in the number of density seems to be not large, but considering the relatively large (e.g. >4 nm) and small particle (e.g. <1 nm) could be catalytically less active, the overall drop in the productive efficiency is significant. Moreover, the density of cobalt nanoparticles formed at 600°C could be estimated from Figure 5 as 1.8E4 $\mu m^{-2}$ by counting the number of particles in a selected area. This density is about as twice as the number density of a typical VA-SWCNT, [31] which suggests the roughly 50% of the catalyst is kept active in the current condition. It explains why vertical forests can be produced. From these *in situ* obtained images, it is clear to discover the reason of monometallic Co yields narrow-diameter distributed and high density SWCNT forests only at 600°C but gives random SWCNT networks at a high temperature, e.g. 800°C.

Another conclusion we learned from the high temperature experiment is shown in Figure 5c and 5d. One long-standing question for the synthesis of SWCNTs is the phase of catalyst during the growth process. And many researchers believe CNT growth follows a vapor liquid solid (VLS) model, in which catalytic particles are liquid at the growth temperature. However, SAED patterns and the enlarged STEM image of the particles in Figure 5c and 5d suggest that our monometallic Co catalyst does not undergo a noticeable melting process or phase change. Diffraction and lattice fringe are routinely observed both when the catalyst just reached 800°C and when catalyst is kept at high temperature over 1 hr. In the enlarged STEM image, furthermore, no surface melting was obtained in this experiment. Though we acknowledge that there could be a slight difference (mostly $H_2$ pressure) in the atmosphere between an *in situ* TEM and real CVD furnace, this difference should be not significant in our case as our standard CVD is also conducted under low pressure. Therefore, so far as we understand, the current study is one of the best attempts in terms of reproducing the condition in a real CVD chamber. The knowledge obtained here reasonably explains why high efficiency and the narrow diameter distribution SWCNTs arrays are obtained only at a low reaction temperature regardless.

The mechanism for different catalyst geometries at different temperatures is briefly discussed here. In classic heterocatalyst, the coarsening of supported metal nanoparticles at elevated temperatures is one dominant mechanism for catalyst deactivation. The size

increase, which is caused by catalyst aggregation or Ostwald ripening [21, 32], results in a loss of the active surface area of the catalyst particle [33]. In the former case, migration and coalescence is the random movement of whole particles on a substrate. When a particle collide with another, they can merge to form a single and larger particle [34]. In the latter case, however, Ostwald ripening describes the loss of surface atoms from small immobile nanoparticles to large nanoparticles [35]. The consequence in common for these two processes is that average particle size increases, where the difference is that ripening causes an additional broadening of size distribution since small particles shrink before they fully give atoms to adjacent larger particles. Lastly we present an extra *in situ* TEM observation at the same location of a catalyst region before and after annealing to study the size change of nanoparticles at high temperatures. Figure S4 (a) and (b) show the TEM images taken at the same area with a time gap of 30 min. The red circles on these TEM images indicate the particles whose size increased after annealing, whereas the blue circles show those particles that shrunk. From these TEM images, the positions of the shrinking or enlarging nanoparticles were constant before and after the heating process, which classified the operative mechanism of coarsening in this system as Ostwald ripening. Carbon-coated cobalt catalyst was also prepared from a few second CVD, and similar ripening process was also observed as shown in Figure S4 (c) and (d). A schematic illustration of Ostwald ripening is given in Figure S4 (e). At elevated temperatures, the atoms on the surface of nanoparticles migrate towards large nanoparticles, which results in an increase of the particle size and a broadening of the size distribution. Some previous study suggested the collective result from the diffusion of surface atoms over time can lead to diffusive particle migration [34], which is not observed in our case and may need a further investigation. The data obtained so far clearly supports that ripening is responsible for the particle coarsening and explains the narrower diameter distribution obtained in our new low temperature recipe. The more dynamic studies are not presented here as we noticed some damages to the catalyst when the same region is exposed to electron beam for a long time. More efforts are still needed to understand the ripening behavior of nanoparticles in real CVD conditions.

## 4. Conclusions

Three significances of the current study are summarized here as conclusions. 1) A new recipe for producing forest-like VA-SWCNT arrays is presented. In this recipe, the catalyst is simplified as monometallic Co and growth temperature is reduced to 600°C. This mild CVD condition can increase the compatibility of synthesizing SWCNT onto other substrates or combining with processes that cannot tolerate a high reaction temperature. 2) The mechanism of successfully combining low temperature and monometallic catalyst for high efficiency growth is investigated by our unique in-plane TEM technique. *Ex situ* TEM reveals the geometry of catalyst particles directly on a $SiO_2$ film, while *in situ* TEM studies at high temperatures visualize the catalyst ripening at a single particle level, and confirms the catalytic particles are in solid phase. These observations satisfactorily explain the high efficiency after combing two previous unfavorable growth conditions, and will benefit the design of new catalyst. 3) The as-synthesized SWCNTs obtained from this new recipe have a narrower diameter distribution than those obtained in previous studies, with 85% of the SWCNTs between 1.6 and 2.4 nm. These arrays with narrow diameter distribution are expected to improve the performance of SWCNTs in many applications. Finally, one drawback of current recipe is that SWCNTs have more defects due to the low synthesis temperature. The quality can be decently improved by balancing the feeding of the carbon source, but a more systematic optimization of parameters (like gas composition, gas velocity, or catalyst pretreatment) is necessary to fully address this problem in the future.

**Acknowledgements**

Part of this work is financially supported by JSPS KAKENHI Grant Numbers JP25107002, JP15H05760, JP15K17984, JP16K05948, JP16H06333, 17K14601, 18H05329, IRENA Project by JST-EC DG RTD, Strategic International Collaborative Research Program, SICORP, and by the “Nanotechnology Platform” of the Ministry of Education, Culture, Sports, Science and Technology (MEXT), Japan. The TEM/STEM work was conducted at Advanced Characterization Nanotechnology Platform of the University of Tokyo.

## References

[1] S. Iijima, T. Ichihashi, Single-shell carbon nanotubes of 1-nm diameter, Nature 363(6430) (1993) 603-605.
[2] R. Saito, M. Fujita, G. Dresselhaus, M.S. Dresselhaus, Electronic-Structure of Chiral Graphene Tubules, Appl Phys Lett 60(18) (1992) 2204-2206.
[3] M.F.L. De Volder, S.H. Tawfick, R.H. Baughman, A.J. Hart, Carbon Nanotubes: Present and Future Commercial Applications, Science 339(6119) (2013) 535-539.
[4] Y. Murakami, S. Chiashi, Y. Miyauchi, M.H. Hu, M. Ogura, T. Okubo, S. Maruyama, Growth of vertically aligned single-walled carbon nanotube films on quartz substrates and their optical anisotropy, Chemical Physics Letters 385(3-4) (2004) 298-303.
[5] S. Maruyama, R. Kojima, Y. Miyauchi, S. Chiashi, M. Kohno, Low-temperature synthesis of high-purity single-walled carbon nanotubes from alcohol, Chemical physics letters 360(3) (2002) 229-234.
[6] K. Hata, D.N. Futaba, K. Mizuno, T. Namai, M. Yumura, S. Iijima, Water-Assisted Highly Efficient Synthesis of Impurity-Free Single-Walled Carbon Nanotubes, Science 306(5700) (2004) 1362-1364.
[7] M.H. Hu, Y. Murakami, M. Ogura, S. Maruyama, T. Okubo, Morphology and chemical state of Co-Mo catalysts for growth of single-walled carbon nanotubes vertically aligned on quartz substrates, Journal of Catalysis 225(1) (2004) 230-239.
[8] M. Fouquet, B.C. Bayer, S. Esconjauregui, R. Blume, J.H. Warner, S. Hofmann, R. Schlögl, C. Thomsen, J. Robertson, Highly chiral-selective growth of single-walled carbon nanotubes with a simple monometallic Co catalyst, Physical Review B 85(23) (2012) 235411.
[9] C.T. Wirth, B.C. Bayer, A.D. Gamalski, S. Esconjauregui, R.S. Weatherup, C. Ducati, C. Baehtz, J. Robertson, S. Hofmann, The Phase of Iron Catalyst Nanoparticles during Carbon Nanotube Growth, Chemistry of Materials 24(24) (2012) 4633-4640.
[10] H. Sugime, S. Noda, Millimeter-tall single-walled carbon nanotube forests grown from ethanol, Carbon 48(8) (2010) 2203-2211.
[11] D.N. Futaba, K. Hata, T. Yamada, K. Mizuno, M. Yumura, S. Iijima, Kinetics of water-assisted single-walled carbon nanotube synthesis revealed by a time-evolution analysis, Physical review letters 95(5) (2005) 056104.
[12] T. Yamada, A. Maigne, M. Yudasaka, K. Mizuno, D.N. Futaba, M. Yumura, S. Iijima, K. Hata, Revealing the secret of water-assisted carbon nanotube synthesis by microscopic observation of the interaction of water on the catalysts, Nano letters 8(12) (2008) 4288-4292.
[13] Y. Murakami, S. Chiashi, Y. Miyauchi, M. Hu, M. Ogura, T. Okubo, S. Maruyama, Growth of vertically aligned single-walled carbon nanotube films on quartz substrates and their optical anisotropy, Chemical Physics Letters 385(3-4) (2004) 298-303.
[14] K. Cui, A. Kumamoto, R. Xiang, H. An, B. Wang, T. Inoue, S. Chiashi, Y. Ikuhara, S. Maruyama, Synthesis of subnanometer-diameter vertically aligned single-walled carbon nanotubes with copper-anchored cobalt catalysts, Nanoscale 8(3) (2016) 1608-1617.
[15] C.J. Lee, S.C. Lyu, Y.R. Cho, J.H. Lee, K.I. Cho, Diameter-controlled growth of carbon nanotubes using thermal chemical vapor deposition, Chemical Physics Letters 341(3-4) (2001) 245-249.
[16] J.I. Sohn, C.-J. Choi, S. Lee, T.-Y. Seong, Growth behavior of carbon nanotubes on Fe-deposited (001) Si substrates, Applied Physics Letters 78(20) (2001) 3130-3132.
[17] P. Chen, H.B. Zhang, G.D. Lin, Q. Hong, K.R. Tsai, Growth of carbon nanotubes by catalytic decomposition of CH4 or CO on a Ni・MgO catalyst, Carbon 35(10) (1997) 1495-1501.

[18] M. Dresselhaus, G. Dresselhaus, Avouris Ph 2001 Carbon Nanotubes: Synthesis, Structure, Properties, and Applications (Berlin: Springer).
[19] J. Kong, A.M. Cassell, H. Dai, Chemical vapor deposition of methane for single-walled carbon nanotubes, Chemical Physics Letters 292(4-6) (1998) 567-574.
[20] D. Takagi, Y. Homma, H. Hibino, S. Suzuki, Y. Kobayashi, Single-walled carbon nanotube growth from highly activated metal nanoparticles, Nano letters 6(12) (2006) 2642-2645.
[21] T.W. Hansen, A.T. DeLaRiva, S.R. Challa, A.K. Datye, Sintering of Catalytic Nanoparticles: Particle Migration or Ostwald Ripening?, Accounts of Chemical Research 46(8) (2013) 1720-1730.
[22] E. Ruckenstein, B. Pulvermacher, Kinetics of Crystallite Sintering during Heat-Treatment of Supported Metal-Catalysts, Aiche J 19(2) (1973) 356-364.
[23] R.T.K. Baker, The Relationship between Particle Motion on a Graphite Surface and Tammann Temperature, Journal of Catalysis 78(2) (1982) 473-476.
[24] R. Xiang, S. Maruyama, Revisiting behaviour of monometallic catalysts in chemical vapour deposition synthesis of single-walled carbon nanotubes, Royal Society Open Science 5(8) (2018) 180345.
[25] B. Hou, C. Wu, T. Inoue, S. Chiashi, R. Xiang, S. Maruyama, Extended alcohol catalytic chemical vapor deposition for efficient growth of single-walled carbon nanotubes thinner than (6, 5), Carbon 119 (2017) 502-510.
[26] R. Xiang, E. Einarsson, Y. Murakami, J. Shiomi, S. Chiashi, Z.K. Tang, S. Maruyama, Diameter Modulation of Vertically Aligned Single-Walled Carbon Nanotubes, Acs Nano 6(8) (2012) 7472-7479.
[27] P.T. Araujo, S.K. Doorn, S. Kilina, S. Tretiak, E. Einarsson, S. Maruyama, H. Chacham, M.A. Pimenta, A. Jorio, Third and fourth optical transitions in semiconducting carbon nanotubes, Physical Review Letters 98(6) (2007) 067401.
[28] M.S. Dresselhaus, G. Dresselhaus, R. Saito, A. Jorio, Raman spectroscopy of carbon nanotubes, Physics reports 409(2) (2005) 47-99.
[29] K. Sato, R. Saito, A.R. Nugraha, S. Maruyama, Excitonic effects on radial breathing mode intensity of single wall carbon nanotubes, Chemical Physics Letters 497(1-3) (2010) 94-98.
[30] H. An, A. Kumamoto, H. Takezaki, S. Ohyama, Y. Qian, T. Inoue, Y. Ikuhara, S. Chiashi, R. Xiang, S. Maruyama, Chirality specific and spatially uniform synthesis of single-walled carbon nanotubes from a sputtered Co–W bimetallic catalyst, Nanoscale 8(30) (2016) 14523-14529.
[31] R. Xiang, Z. Yang, Q. Zhang, G. Luo, W. Qian, F. Wei, M. Kadowaki, E. Einarsson, S. Maruyama, Growth deceleration of vertically aligned carbon nanotube arrays: Catalyst deactivation or feedstock diffusion controlled?, The Journal of Physical Chemistry C 112(13) (2008) 4892-4896.
[32] C.H. Bartholomew, Mechanisms of catalyst deactivation, Applied Catalysis A: General 212(1) (2001) 17-60.
[33] D. Kistamurthy, A.M. Saib, D.J. Moodley, J.W. Niemantsverdriet, C.J. Weststrate, Ostwald ripening on a planar Co/SiO2 catalyst exposed to model Fischer–Tropsch synthesis conditions, Journal of Catalysis 328 (2015) 123-129.
[34] P. Wynblatt, N. Gjostein, Supported metal crystallites, Progress in solid state chemistry 9 (1975) 21-58.
[35] B.K. Chakraverty, Grain size distribution in thin films—1. Conservative systems, Journal of Physics and Chemistry of Solids 28(12) (1967) 2401-2412.

**Supporting information**

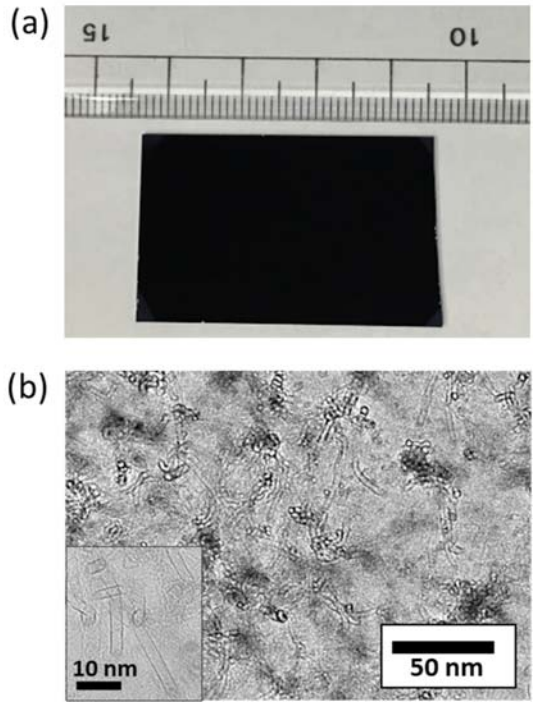


Figure S1 Optical image of a vertical aligned SWCNT array grown on a substrate. (b) Top view TEM image of the SWCNT array, showing the clear crossections of isolated and bundled SWCNTs. Inset shows side view TEM image of the SWCNTs.

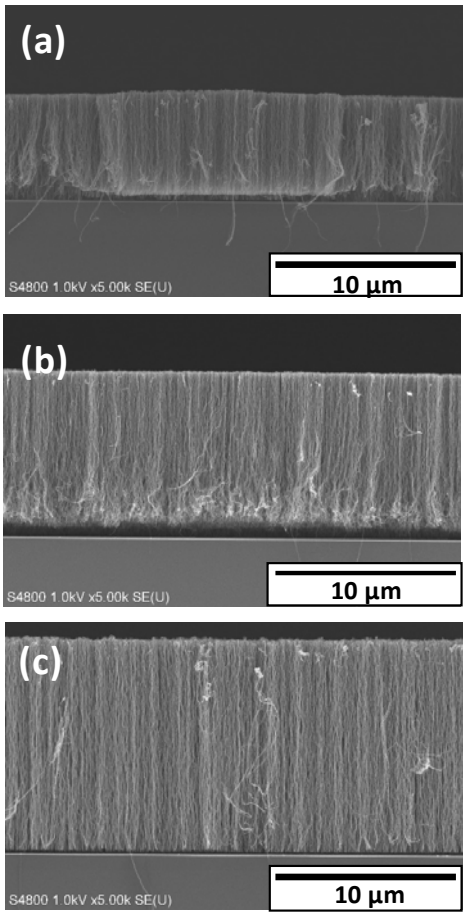


Figure S2. Representative SEM images of VA-SWCNTs synthesized at different ethanol flow rates: (a) 50, (b) 250, and (c) 450 sccm.

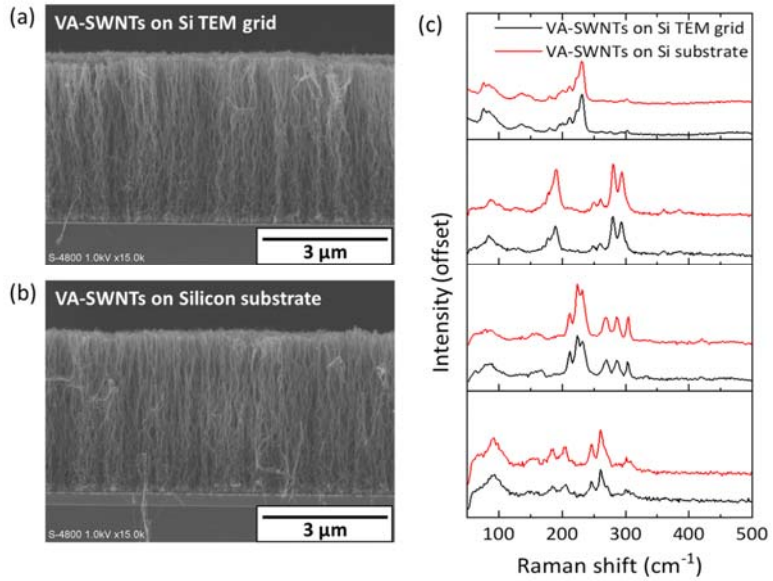


Figure S3. Representative SEM images of VA-SWCNTs synthesized (a) on Si TEM grid; (b) on silicon substrate. (c) Representative Raman spectra of VA-SWCNTs synthesized on Si TEM grid and silicon substrate measured by laser excitation at 488, 532, 633, and 785 nm.

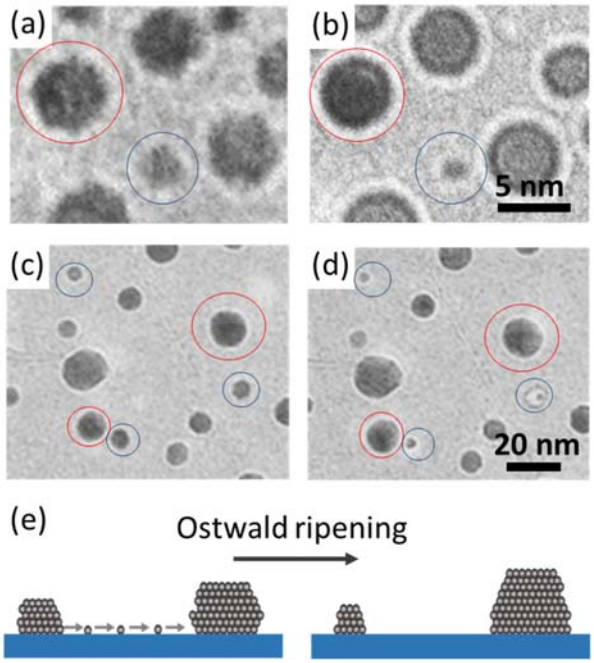


Figure S4. Characterization of catalyst ripening at single particle level. Representative TEM images of (a) metallic cobalt catalyst, (b) metallic cobalt catalyst after annealing at 850°C for 30 min, (c) carbon-coated cobalt catalyst, and (d) carbon-coated cobalt catalyst after annealing at 850°C for 30 min. (e) Schematic illustration of Ostwald ripening.